

Probing τ lepton dipole moments at future Lepton Colliders

Dario Buttazzo¹, Gabriele Levati², Yang Ma³, Fabio Maltoni^{3,4,5}, Paride Paradisi^{6,7} and ZeQiang Wang³

¹*Istituto Nazionale di Fisica Nucleare, Sezione di Pisa, I-56127 Pisa, Italy*

²*Albert Einstein Center for Fundamental Physics, Institute for Theoretical Physics, University of Bern, Sidlerstrasse 5, 3012 Bern, Switzerland*

³*Centre for Cosmology, Particle Physics and Phenomenology (CP3), UCLouvain, 1348 Louvain-la-Neuve, Belgium*

⁴*Dipartimento di Fisica e Astronomia, Università di Bologna and INFN, Sezione di Bologna, via Irnerio 46, 40126 Bologna, Italy*

⁵*CERN, Theoretical Physics Department, CH-1211 Geneva 23, Switzerland*

⁶*Dipartimento di Fisica e Astronomia ‘G. Galilei’, Università di Padova, Italy*

⁷*Istituto Nazionale Fisica Nucleare, Sezione di Padova, I-35131 Padova, Italy*

The electric and magnetic dipole moments of the electron and of the muon provide stringent tests of the Standard Model and sensitive probes of new physics. By contrast, the corresponding dipole moments of the τ lepton remain weakly constrained. This study explores the potential of future lepton colliders, focusing on the e^+e^- Future Circular Collider and a multi-TeV muon collider, to probe τ dipole moments. We consider multiple channels, including $\ell^+\ell^- \rightarrow \tau^+\tau^-$ ($\ell = e, \mu$), associated Higgs production $\mu^+\mu^- \rightarrow \tau^+\tau^-H$, radiative Higgs decays $H \rightarrow \tau^+\tau^-\gamma$, and vector-boson scattering $\ell^+\ell^- \rightarrow \ell^+\ell^-\tau^+\tau^-$ and $\mu^+\mu^- \rightarrow \bar{\nu}\nu\tau^+\tau^-$. Our results show that these facilities are highly complementary and can extend existing bounds by several orders of magnitude.

I. INTRODUCTION

Since the discovery of the Higgs boson at the LHC, no direct evidence for new physics (NP) has emerged at the TeV scale. Inspired by historical precedents in high-energy physics where new particles first manifested through virtual effects, the precision frontier has become a primary avenue to probe NP dynamics via deviations from high-precision Standard Model (SM) predictions.

Lepton dipole moments are among the most sensitive SM tests and provide powerful indirect probes of NP. The electron and muon anomalous magnetic moments a_ℓ ($\ell = e, \mu$) are measured with high precision [1–3]. Matching theoretical accuracy is crucial to maximize sensitivity to NP: for a_e , the dominant uncertainty stems from the fine-structure constant [4, 5], while for a_μ it is driven by hadronic vacuum polarization, with recent progress from lattice QCD [6]. The current comparison between theory and experiment shows no significant discrepancy [6], motivating further reduction of theoretical errors [6, 7] to fully exploit the experimental sensitivity. In contrast, the electron and muon electric dipole moments d_ℓ are negligible in the SM; any signal below current bounds [8, 9] would constitute clear evidence of CP-violating NP.

The τ lepton case is different. Its short lifetime prevents direct measurements of a_τ and d_τ in external electromagnetic fields, as for the electron and muon. They must therefore be inferred from high-energy τ -pair production via precise comparisons between measured cross sections and SM predictions. The SM prediction for the τ anomalous magnetic moment, $a_\tau^{\text{SM}} = 117717.1(4.0) \times 10^{-8}$ [10–14], has an uncertainty well below any foreseeable experimental sensitivity. Precise measurements of a_τ and d_τ would therefore provide a unique probe of NP, particularly in scenarios with enhanced couplings to

third-generation fermions, as expected in models addressing the SM flavor structure [15–27].

Deviations of the τ dipole moments from their SM values, induced by NP dynamics at a scale Λ well above the electroweak scale, can be described within an effective field theory (EFT) approach. The SM Lagrangian is extended by a set of gauge-invariant higher-dimensional operators constructed from SM fields and suppressed by appropriate powers of Λ [28]. In this framework, the DELPHI Collaboration at LEP-II reported the 95% C.L. limits on the τ dipole moments, obtained via photon-photon collisions $\gamma\gamma \rightarrow \tau^+\tau^-$, yielding $-0.052 < a_\tau < 0.013$ and $|d_\tau| < 3.7 \times 10^{-16} e \text{ cm}$ [29]. At the LHC, recent measurements by the ATLAS [30] and CMS [31] Collaborations have significantly improved these constraints, resulting in $a_\tau \in [-2.4, 4.7] \times 10^{-3}$ and $|d_\tau| < 2.0 \times 10^{-17} e \text{ cm}$ at 95% C.L. [30]. The projected sensitivity of the High-Luminosity LHC to a_τ and d_τ is expected to provide only a modest improvement over current bounds, reaching the level of $a_\tau \sim \mathcal{O}(10^{-3})$ and $|d_\tau| \sim \mathcal{O}(10^{-17}) e \text{ cm}$.

The most stringent constraint on the τ electric dipole moment, $d_\tau \in [-1.85, 0.61] \times 10^{-17} e \text{ cm}$ at 95% C.L., has been reported by the Belle II Collaboration [32], while no corresponding limit on a_τ has yet been established. More ambitious strategies exploiting asymmetries in $e^+e^- \rightarrow \tau^+\tau^-$ [33–35] and assuming an integrated luminosity of 50 ab^{-1} are being pursued at Belle II, targeting projected sensitivities of $|a_\tau| \lesssim 10^{-5}$ and $|d_\tau| \lesssim 10^{-19} e \text{ cm}$ [36–42].

In this Letter, we examine the prospects for measuring the τ dipole moments at future high-energy lepton colliders, focusing on the e^+e^- Future Circular Collider (FCC-ee) [43–46] and a multi-TeV Muon Collider (μC) [47–58]. These facilities offer complementary capabilities: FCC-ee enables high-precision studies of the Higgs, W , and Z bosons, while a high-energy μC extends the energy fron-

tier, providing direct access to heavy-particle production.

Owing to its very high luminosity, the FCC-ee will achieve unprecedented sensitivity to indirect NP effects in tiny deviations from SM predictions in electroweak precision observables, far beyond the LEP resolutions. Therefore, we investigate the yet unexplored potential to improve the LEP determination of a_τ and d_τ at FCC-ee. As at LEP, the FCC-ee can probe τ dipole moments via direct $\tau^+\tau^-$ production in $e^+e^- \rightarrow \tau^+\tau^-$ and in photon-photon collisions $\gamma\gamma \rightarrow \tau^+\tau^-$. Moreover, as a Higgs factory, the FCC-ee provides a clean experimental environment and allows for precise Higgs reconstruction. Despite a comparatively smaller Higgs sample, $\mathcal{O}(10^6)$, than that available at the LHC, it affords a unique sensitivity to the τ magnetic dipole moment via $H \rightarrow \tau^+\tau^-\gamma$ [59].

We observe that dipole operators contribute to $\mu^+\mu^- \rightarrow \tau^+\tau^-H$ through the $H\tau^+\tau^-\gamma^*$ vertex. Although the latter process is phase-space suppressed with respect to $\mu^+\mu^- \rightarrow \tau^+\tau^-$, it features a stronger energy growth of NP effects, and may therefore provide enhanced NP sensitivity at multi-TeV energies. Moreover, since a significantly larger Higgs yield than at FCC-ee is expected at a μ C operating at $\mathcal{O}(10 \text{ TeV})$, $H \rightarrow \tau^+\tau^-\gamma$ is a sensitive probe of τ dipole moments also at a high-energy μ C. Finally, the vector-boson-scattering (VBS) channels $\mu^+\mu^- \rightarrow \mu^+\mu^-\tau^+\tau^-$ and $\mu^+\mu^- \rightarrow \bar{\nu}\nu\tau^+\tau^-$ are also sensitive to the τ dipole moments through the exchange of electroweak gauge bosons.

II. TAU DIPOLE MOMENTS IN THE SMEFT

New interactions at a scale Λ above the electroweak scale can be described, for energies $E \ll \Lambda$, by an effective Lagrangian containing non-renormalizable operators invariant under the SM gauge group $SU(3)_c \otimes SU(2)_L \otimes U(1)_Y$. Focusing on leptonic dipole operators, the relevant effective Lagrangian reads [28, 60]:

$$\mathcal{L} \supset \bar{\ell}_L \sigma^{\mu\nu} e_R \left(\frac{\mathcal{C}_{\ell B}}{\Lambda^2} \varphi B_{\mu\nu} + \frac{\mathcal{C}_{\ell W}}{\Lambda^2} \tau^I \varphi W_{\mu\nu}^I \right) + \text{h.c.} \quad (1)$$

where φ contains both the Higgs field H and its vacuum expectation value $v = 246 \text{ GeV}$, and $B_{\mu\nu}$ and $W_{\mu\nu}^I$ denote the $U(1)_Y$ and $SU(2)_L$ field-strength tensors.

Within an EFT framework, perturbative unitarity sets an upper bound on the energy scale at which scattering amplitudes become nonperturbative, with a detailed analysis of the operators in Eq. (1) yielding [61, 62]

$$s \frac{|\mathcal{C}_{\ell B}|}{\Lambda^2} < 4\pi, \quad s \frac{|\mathcal{C}_{\ell W}|}{\Lambda^2} < 4\pi \sqrt{2/3}. \quad (2)$$

After electroweak symmetry breaking, Eq. (1) generates tree-level effects to electromagnetic dipole moments:

$$\Delta a_\tau \simeq \frac{4m_\tau v}{e\sqrt{2}\Lambda^2} \text{Re } \mathcal{C}_{\tau\gamma}, \quad d_\tau \simeq \frac{2v}{\sqrt{2}\Lambda^2} \text{Im } \mathcal{C}_{\tau\gamma}, \quad (3)$$

where $\mathcal{C}_{\tau\gamma} = c_W \mathcal{C}_{\tau B} - s_W \mathcal{C}_{\tau W}$ and $s_W(c_W)$ is the sine (cosine) of the weak mixing angle. Moreover, via the coupling to the Z boson, Eq. (1) also generates NP contributions to the neutral weak dipole moments, Δa_τ^Z and d_τ^Z . These are obtained from Δa_τ and d_τ in Eq. (3) by replacing $\mathcal{C}_{\tau\gamma}$ with $\mathcal{C}_{\tau Z}$, where $\mathcal{C}_{\tau Z} = -s_W \mathcal{C}_{\tau B} - c_W \mathcal{C}_{\tau W}$.

To assess the benchmark sensitivity that can be obtained at colliders, we can determine the NP scale that can be probed through Δa_τ . From Eq. (3), we obtain

$$\Delta a_\tau \approx 3.7 \times 10^{-5} \left(\frac{10 \text{ TeV}}{\Lambda} \right)^2 \text{Re } \mathcal{C}_{\tau\gamma}, \quad (4)$$

where $\mathcal{C}_{\tau\gamma}$ has been evaluated at the scale m_τ by including its one-loop renormalization effects [63–67].

A few comments are in order:

- $\Delta a_\tau \sim \mathcal{O}(10^{-4})$ can be achieved for $\Lambda \approx 10 \text{ TeV}$ and $\text{Re } \mathcal{C}_{\tau\gamma} \sim 1$, indicating a strongly coupled NP sector where $\text{Re } \mathcal{C}_{\tau\gamma} \sim g_{\text{NP}}^2/(16\pi^2) \sim 1$. This scenario further requires a chiral enhancement factor v/m_τ relative to the naive scaling $\Delta a_\tau \propto m_\tau^2$ [68].
- If the NP sector is weakly coupled, i.e., $g_{\text{NP}} \sim 1$, but still exhibits a chiral enhancement, $\Delta a_\tau \sim 10^{-4}$ can be realized for a NP scale of $\Lambda \approx 1 \text{ TeV}$.
- Weakly coupled NP scenarios without chiral enhancement can generate $\Delta a_\tau \sim 10^{-4}$ only for a light NP scale $\Lambda \lesssim v$, which is strongly disfavored by direct searches at LEP and the LHC.¹

In Fig. 1, we show the most relevant processes sensitive to τ dipole moments at FCC-ee and a μ C. The dipole operators in Eq. (1) induce a $\tau^+\tau^-HV$ vertex ($V = \gamma, Z$), which mediates both the decay $H \rightarrow \tau^+\tau^-\gamma$ and the associated production process $\ell^+\ell^- \rightarrow \tau^+\tau^-H$.

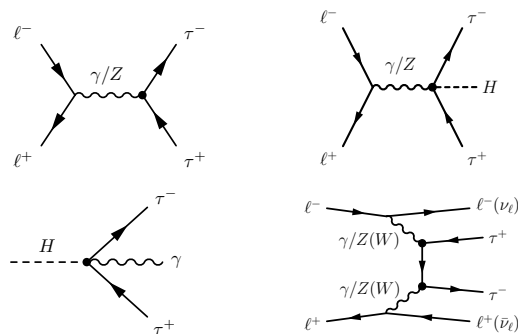


FIG. 1. Processes sensitive to τ dipole moments at the FCC-ee and a muon collider (representative Feynman diagrams).

¹Effects from a very light NP sector ($\Lambda \lesssim 1 \text{ GeV}$) feebly coupled to SM particles remain allowed [40, 41, 69, 70].

III. TAU DIPOLE MOMENTS AT FCC-EE

We now analyze the sensitivity to the τ dipole moments at FCC-ee, see Fig. 1, assuming the expected integrated luminosities reported in Table I.

We first consider the process $\ell^+\ell^- \rightarrow \tau^+\tau^-$ ($\ell = e, \mu$), for which the total cross section, $\sigma_{\ell\ell}$, can be cast as $\sigma_{\ell\ell} = \sigma_{\ell\ell}^{\text{SM}} + \sigma_{\ell\ell}^{\text{Lin}} + \sigma_{\ell\ell}^{\text{Quad}}$, where $\sigma_{\ell\ell}^{\text{Lin}}$ arises from the interference between the SM and NP contributions while $\sigma_{\ell\ell}^{\text{Quad}}$ is the pure NP effect. In particular, we obtain

$$\sigma_{\ell\ell}^{\text{SM}} = \frac{\beta}{12\pi} \left[\frac{e^4(1+2\tau)}{s} + \frac{2e^2g_Z^2g_V^2s\Delta(1+2\tau)}{\Delta^2s^2 + M_Z^2\Gamma_Z^2} + \frac{g_Z^4s(g_V^2 + g_A^2)(g_V^2(1+2\tau) + g_A^2(1-4\tau))}{\Delta^2s^2 + M_Z^2\Gamma_Z^2} \right], \quad (5a)$$

$$\sigma_{\ell\ell}^{\text{Lin}} = \frac{\beta m_\tau v}{\sqrt{2}\pi s \Lambda^2} \text{Re} \left[e^3 C_{\tau\gamma} + \frac{eg_Z^2g_V^2 C_{\tau\gamma} \Delta s^2}{\Delta^2s^2 + M_Z^2\Gamma_Z^2} - \frac{gzg_V C_{\tau Z} s^2 (e^2\Delta + g_Z^2(g_V^2 + g_A^2))}{\Delta^2s^2 + M_Z^2\Gamma_Z^2} \right], \quad (5b)$$

$$\sigma_{\ell\ell}^{\text{Quad}} = \frac{\beta v^2(1+8\tau)}{12\pi\Lambda^4} \left[e^2 |C_{\tau\gamma}|^2 + \frac{g_Z^2 |C_{\tau Z}|^2 s^2 (g_V^2 + g_A^2)}{\Delta^2s^2 + M_Z^2\Gamma_Z^2} - \frac{2eg_Zg_V \text{Re}(C_{\tau\gamma}^* C_{\tau Z}) \Delta s^2}{\Delta^2s^2 + M_Z^2\Gamma_Z^2} \right], \quad (5c)$$

where $\tau = m_\tau^2/s$, $\beta = \sqrt{1-4\tau}$, and $\Delta = 1 - M_Z^2/s$. The weak couplings are defined as $g_Z = g/c_W$, $g_V = -1/4 + s_W^2$, and $g_A = -1/4$. Due to the helicity-flipping structure of the NP amplitude relative to the SM one, the interference term is suppressed by $m_\tau v/s$. Therefore, quadratic contributions dominate at high energies, while linear terms set the sensitivity at low energies.

Working point	Z pole	WW	ZH	tt
\sqrt{s} [GeV]	87.9, 91.2, 94.3	157.5, 162.5	240	365
\mathcal{L} [ab ⁻¹]	40, 125, 40	9.6, 9.6	10.8	2.7

TABLE I. Center of mass energies, \sqrt{s} , and integrated luminosities, \mathcal{L} , at FCC-ee [45] in the stages of a Tera-Z (Z pole), electroweak (WW), Higgs (ZH), and top (tt) factories.

Assuming the FCC-ee benchmark points listed in Table I, Fig. 2 shows the 95% CL bounds in the $(C_{\tau\gamma}, C_{\tau Z})$ plane from the process $e^+e^- \rightarrow \tau^+\tau^-$. The upper plot corresponds to center-of-mass energies $\sqrt{s} \simeq M_Z$ (Tera-Z stage), where the dominant NP effects are well captured by the linear contributions. By contrast, the lower plot refers to center-of-mass energies $\sqrt{s} = 2M_W$, 240 GeV, 365 GeV, for which quadratic NP effects become increasingly important as the energy increases. Bounds obtained at different energies are highly complementary, leading to significantly stronger combined constraints.

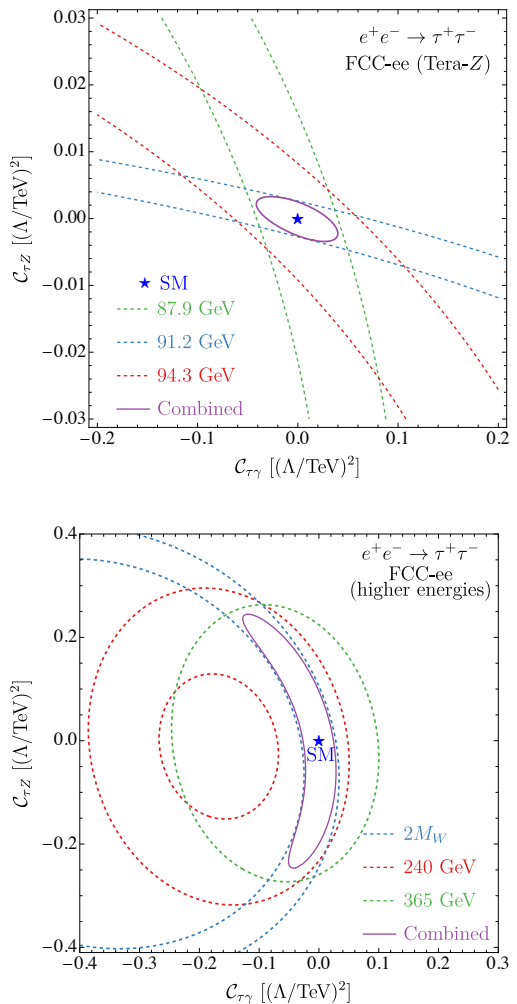


FIG. 2. 95% CL bounds in the $(C_{\tau\gamma}, C_{\tau Z})$ plane at FCC-ee from $e^+e^- \rightarrow \tau^+\tau^-$ for the benchmark points of Table I. The bounds scale as $(\Lambda/\text{TeV})^2$ and assume real $C_{\tau\gamma}$ and $C_{\tau Z}$.

In our numerical analysis, we include initial-state-radiation (ISR) and maximize the signal significance by imposing kinematic cuts on the invariant mass of the τ pair $m(\tau^+\tau^-) > 0.8\sqrt{s}$, the angular separation $\Delta R(\tau^+\tau^-) > 0.4$, and the transverse momentum $p_T(\tau^\pm) > 0.1\sqrt{s}$. Moreover, we assume an 80% τ -reconstruction efficiency. To account for detector acceptance, all final-state particles are required to have polar angles $\theta > 5^\circ$ with respect to the beam axis.

Table II reports the bounds on $\Delta a_\tau^{(Z)}$ and $d_\tau^{(Z)}$ for each FCC-ee reference energy (see Table I) and for the combined limits. It is worth emphasizing that the bounds on both a_τ and a_τ^Z are dominated by Z -pole data at FCC-ee (Tera-Z stage), in contrast to the LEP case, where the strongest bounds were obtained at LEP-II energies. This result stems from the much higher FCC-ee luminosities, which allow linear NP effects to dominate over quadratic ones despite chirality suppression.

\sqrt{s}	$ \Delta a_\tau $	$ \Delta a_\tau^Z $	$ d_\tau [e \cdot \text{cm}]$	$ d_\tau^Z [e \cdot \text{cm}]$
M_Z	1.3×10^{-4}	1.0×10^{-5}	6.0×10^{-18}	4.4×10^{-19}
$2M_W$	1.2×10^{-4}	9.8×10^{-4}	3.3×10^{-18}	3.6×10^{-18}
240 GeV	2.8×10^{-4}	9.3×10^{-4}	3.1×10^{-18}	4.4×10^{-18}
365 GeV	1.0×10^{-3}	1.0×10^{-3}	3.5×10^{-18}	5.5×10^{-18}
Combined	8.2×10^{-5}	1.0×10^{-5}	2.5×10^{-18}	4.4×10^{-19}

TABLE II. 95% CL bounds on $\Delta a_\tau^{(Z)}$ and $d_\tau^{(Z)}$ at FCC-ee from $e^+e^- \rightarrow \tau^+\tau^-$, for $\mathcal{C}_{\tau B}$ and $\mathcal{C}_{\tau W}$ purely real or imaginary.

Within the equivalent photon approximation (EPA), the cross section for $\ell^+\ell^- \rightarrow \ell^+\ell^-\tau^+\tau^-$ is given by the convolution of the photon emission probabilities with the partonic cross section $\hat{\sigma}_{\gamma\gamma}(\hat{s})$ for $\gamma\gamma \rightarrow \tau^+\tau^-$:

$$\sigma_{\gamma\gamma}(s) = \int_{\xi_0}^1 d\xi \int_{\xi}^1 \frac{dx}{x} f_{\gamma/\ell}(x, Q^2) f_{\gamma/\ell}\left(\frac{\xi}{x}, Q^2\right) \hat{\sigma}_{\gamma\gamma}(\hat{s}), \quad (6)$$

where $\xi = \hat{s}/s$, with $\sqrt{\hat{s}}$ the partonic center-of-mass energy, and $\xi_0 = \hat{s}_{\min}/s$ set by the production threshold or kinematic cuts. The photon PDF $f_{\gamma/\ell}(x, Q^2)$, giving the probability for a lepton to emit a photon with momentum fraction x at factorization scale Q , is taken in the improved Weizsäcker–Williams approximation [71].

Retaining contributions up to $1/\Lambda^4$, $\hat{\sigma}_{\gamma\gamma}$ can be expanded as $\hat{\sigma}_{\gamma\gamma} = \hat{\sigma}_{\gamma\gamma}^{\text{SM}} + \hat{\sigma}_{\gamma\gamma}^{\text{Lin}} + \hat{\sigma}_{\gamma\gamma}^{\text{Quad}}$ where

$$\begin{aligned} \hat{\sigma}_{\gamma\gamma}^{\text{SM}} &= \frac{e^4}{4\pi\hat{s}} \left[(1 + 4\hat{\tau} - 8\hat{\tau}^2) \log\left(\frac{1 + \hat{\beta}}{1 - \hat{\beta}}\right) - \hat{\beta}(1 + 4\hat{\tau}) \right], \\ \hat{\sigma}_{\gamma\gamma}^{\text{Lin}} &= \frac{\sqrt{2}e^3 m_\tau v \text{Re}\mathcal{C}_{\tau\gamma}}{\pi\hat{s} \Lambda^2} \log\left(\frac{1 + \hat{\beta}}{1 - \hat{\beta}}\right), \\ \hat{\sigma}_{\gamma\gamma}^{\text{Quad}} &= \frac{e^2 v^2 |\mathcal{C}_{\tau\gamma}|^2}{\pi \Lambda^4} \left[\hat{\tau} \log\left(\frac{1 + \hat{\beta}}{1 - \hat{\beta}}\right) + 2\hat{\beta} \right], \end{aligned} \quad (7)$$

with $\hat{\tau} = m_\tau^2/\hat{s}$ and $\hat{\beta} = \sqrt{1 - 4m_\tau^2/\hat{s}}$. Unlike $e^+e^- \rightarrow \tau\tau$, the $\gamma\gamma \rightarrow \tau\tau$ cross section is dominated by low- \hat{s} interactions, where the $m_\tau v/\hat{s}$ suppression is reduced. As a result, the linear NP contribution remains dominant over the full accessible energy range.

τ -pair production in photon-photon collisions was studied at LEP-II by the DELPHI Collaboration using $\sim 650 \text{ pb}^{-1}$ of data at $\sqrt{s} = 183\text{--}208 \text{ GeV}$ [29]. Expected signal yields are computed using the foreseen FCC-ee integrated luminosities and the $\tau^+\tau^-$ reconstruction efficiencies reported by DELPHI for their 1997–1999 data-taking period [29], providing a conservative yet reliable benchmark for projecting event rates and signal significance at future e^+e^- colliders.

In the top panel of Fig. 3, we show the 95% CL bounds in the $(\mathcal{C}_{\tau W}, \mathcal{C}_{\tau B})$ plane from the process $\gamma\gamma \rightarrow \tau^+\tau^-$, assuming the FCC-ee benchmark points listed in Table I. The strongest constraints, aligned entirely along the $\mathcal{C}_{\tau\gamma}$ direction, originate from linear NP effects and are obtained at $\sqrt{s} \simeq M_Z$ (Tera- Z stage), thanks to the highest integrated luminosity. In Table III, we report the

95% CL constraints on $|\Delta a_\tau|$ and $|d_\tau|$ from $\gamma\gamma \rightarrow \tau^+\tau^-$. While the combined bound on $|\Delta a_\tau|$ improves by roughly a factor of three compared to $e^+e^- \rightarrow \tau^+\tau^-$, the latter process remains more sensitive to $|d_\tau|$.

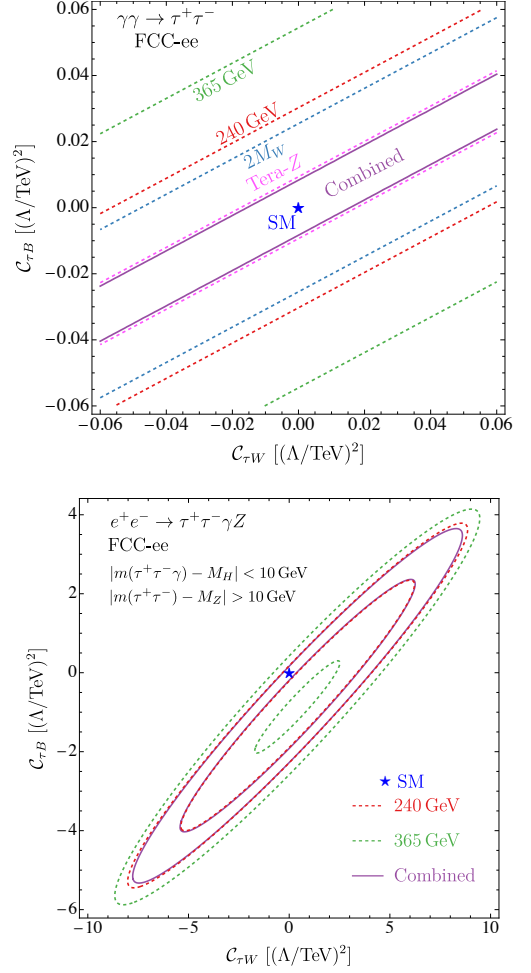


FIG. 3. 95% CL bounds in the $(\mathcal{C}_{\tau W}, \mathcal{C}_{\tau B})$ plane at FCC-ee from $\gamma\gamma \rightarrow \tau^+\tau^-$ (top) and $H \rightarrow \tau^+\tau^-\gamma$ (bottom) for the benchmark points of Table I. The bounds scale as $(\Lambda/\text{TeV})^2$ and assume real $\mathcal{C}_{\tau W}$ and $\mathcal{C}_{\tau B}$.

\sqrt{s}	M_Z	$2M_W$	240 GeV	365 GeV	Combined
$ \Delta a_\tau $	3.4×10^{-5}	9.2×10^{-5}	1.1×10^{-4}	2.0×10^{-4}	3.0×10^{-5}
$ d_\tau [e \cdot \text{cm}]$	1.7×10^{-17}	2.7×10^{-17}	2.8×10^{-17}	3.6×10^{-17}	1.6×10^{-17}

TABLE III. 95% CL bounds on Δa_τ and d_τ at FCC-ee from $\gamma\gamma \rightarrow \tau^+\tau^-$, for $\mathcal{C}_{\tau B}$ and $\mathcal{C}_{\tau W}$ purely real or imaginary.

Finally, we consider the radiative Higgs decay $H \rightarrow \tau^+\tau^-\gamma$ at FCC-ee, arising from the process $e^+e^- \rightarrow HZ \rightarrow \tau^+\tau^-\gamma Z$. The dipole operators in Eq. (1) contribute to the decay width as [59]

$$\Gamma(H \rightarrow \tau^+\tau^-\gamma)_{\text{NP}} = \frac{ey_\tau M_H^3 \text{Re}\mathcal{C}_{\tau\gamma}}{64\pi^3 \Lambda^2} + \frac{M_H^5}{768\pi^3} \frac{|\mathcal{C}_{\tau\gamma}|^2}{\Lambda^4}. \quad (8)$$

To isolate this channel, in our numerical analysis we impose a Higgs-mass window $|m(\tau^+\tau^-\gamma) - M_H| < 10 \text{ GeV}$

\sqrt{s}	$ \Delta a_\tau $	$ \Delta a_\tau^Z $	$ d_\tau [e \cdot \text{cm}]$	$ d_\tau^Z [e \cdot \text{cm}]$
240 GeV	7.5×10^{-4}	2.0×10^{-2}	1.3×10^{-17}	1.1×10^{-16}
365 GeV	2.6×10^{-3}	2.9×10^{-2}	2.1×10^{-17}	1.6×10^{-16}
Combined	7.0×10^{-4}	1.9×10^{-2}	1.2×10^{-17}	1.1×10^{-16}

TABLE IV. 95% CL bounds on $\Delta a_\tau^{(Z)}$ and $d_\tau^{(Z)}$ at FCC-ee from $H \rightarrow \tau^+\tau^-\gamma$, for $\mathcal{C}_{\tau B}$ and $\mathcal{C}_{\tau W}$ purely real or imaginary.

and a Z veto, $|m(\tau^+\tau^-) - M_Z| > 10$ GeV, to suppress the dominant background from on-shell Z production. The 95% CL constraints are shown as contours in the $(\mathcal{C}_{\tau W}, \mathcal{C}_{\tau B})$ plane in the bottom panel of Fig. 3, with the related bounds on $\Delta a_\tau^{(Z)}$ and $d_\tau^{(Z)}$ reported in Table IV. Although less constraining than $e^+e^- \rightarrow \tau^+\tau^-$ and $\gamma\gamma \rightarrow \tau^+\tau^-$ (see Tables II and III), the decay $H \rightarrow \tau^+\tau^-\gamma$ at FCC-ee could substantially improve upon current LHC bounds.

IV. TAU DIPOLE MOMENTS AT A μC

We now assess the sensitivity to τ dipole moments at a μC , assuming an integrated luminosity $\mathcal{L} = 10 \text{ ab}^{-1} (\sqrt{s}/10 \text{ TeV})^2$ and benchmark energies $\sqrt{s} = 3, 6, 10, 14$ TeV. For the numerical simulation, we adopt a setup consistent with the FCC-ee analysis. To mitigate beam-induced background, we further impose $\theta > 10^\circ$.

We first consider the process $\mu^+\mu^- \rightarrow \tau^+\tau^-$, which at μC energies is dominated by quadratic NP contributions, see Eq. (5). The resulting 95% CL bounds on Δa_τ and d_τ are shown in Fig. 4. As expected, the reach improves as $1/\sqrt{s}$ with increasing energy, due to the $1/s$ suppression of the SM background relative to the NP signal, see Eq. (5), and the luminosity scaling with energy, $\mathcal{L} \propto s$. This implies that, at sufficiently high energy, $\mu\mu \rightarrow \tau\tau$ reaches the limit of EFT validity. The bounds on Δa_τ remain weaker than the FCC-ee limit, which is dominated by linear NP effects in $\gamma\gamma \rightarrow \tau^+\tau^-$, even at $\sqrt{s} \sim 20$ TeV. By contrast, the limits on d_τ arise from quadratic NP contributions both at FCC-ee and at a μC , so the higher energies of the latter lead to significantly stronger constraints.

The process $\mu^+\mu^- \rightarrow \tau^+\tau^-H$ is described, in the high-energy limit $s \gg M_{H,Z}^2$, by the differential cross section

$$\frac{d\sigma_{\tau\tau H}}{dx_1 dx_2} \simeq \frac{1}{192\pi^3} \frac{s}{\Lambda^4} (1 - x_1 - x_2 + 2x_1 x_2) \cdot [|\mathcal{C}_{\tau\gamma}|^2 e^2 - 2e g_z g_V \text{Re}(\mathcal{C}_{\tau Z}^* \mathcal{C}_{\tau\gamma}) + |\mathcal{C}_{\tau Z}|^2 g_z^2 (g_A^2 + g_V^2)], \quad (9)$$

where $x_i = 2Q \cdot k_i / Q^2$, with k_i the four-momenta of the final-state τ pair and Q the total momentum of the initial muon pair. In addition to the baseline selection cuts used for $\mu^+\mu^- \rightarrow \tau^+\tau^-$, we impose $m(\tau^+\tau^-) > \sqrt{s}/10$ to further suppress the SM background from $\mu^+\mu^- \rightarrow ZH$ with $Z \rightarrow \tau^+\tau^-$. We tag $H \rightarrow b\bar{b}$ with a bottom-tagging efficiency of 80% and assume a 15% misidenti-

fication rate from $Z \rightarrow b\bar{b}$ as $H \rightarrow b\bar{b}$. At high energies, $\mu^+\mu^- \rightarrow \tau^+\tau^-Z$ and $\mu^+\mu^- \rightarrow \tau^\pm \nu_\tau W^\mp$ receive the same NP effects as $\mu^+\mu^- \rightarrow \tau^+\tau^-H$, since the longitudinal W^\pm and Z modes dominate, in agreement with the Goldstone boson equivalence theorem [72–74]. The linear growth with s in Eq. (9), combined with the luminosity scaling $\mathcal{L} \propto s$, results in a reach that scales as $1/s$, see Fig. 4. Notably, this implies that these bounds could be indefinitely improved by raising the center-of-mass energy without violating EFT validity, in contrast to pair production which saturates the unitarity bound at $\sqrt{s} \sim 30$ TeV. The bounds on Δa_τ and d_τ are comparable to those from $\mu^+\mu^- \rightarrow \tau^+\tau^-$ at $\sqrt{s} \sim 2$ TeV and about one order of magnitude stronger at $\sqrt{s} \sim 10$ TeV.

Unlike at FCC-ee, probing τ dipole moments via VBS $\tau^+\tau^-$ production in the linear NP regime is challenging at a μC due to large QCD dijet backgrounds [75]. To isolate the VBS contribution from muon annihilation and maximize NP sensitivity, we impose $p_T(\tau^\pm) > 0.1 x\sqrt{s}$ and an invariant-mass window $x\sqrt{s} < m(\tau^+\tau^-) < 0.8\sqrt{s}$, with x optimized for each \sqrt{s} (typically $x = 0.2-0.3$). Experimentally, separating pure VBS from $\mu^+\mu^- \rightarrow \tau^+\tau^-Z$ with $Z \rightarrow \nu\bar{\nu}$ is challenging, leading to a reach scaling as $1/s$ at high energies (see Fig. 4).

The μC also operates as a powerful Higgs factory, with W^+W^- fusion producing $\mathcal{O}(10^7)$ Higgs bosons at $\sqrt{s} \sim 10$ TeV. We simulate the full processes $\mu^+\mu^- \rightarrow \tau^+\tau^-\gamma + \mu^+\mu^-/\nu\bar{\nu}$ to capture the radiative Higgs decay $H \rightarrow \tau^+\tau^-\gamma$. To isolate this channel, we impose Higgs-mass and Z -veto selection cuts as in the FCC-ee analysis, together with an additional $p_T > \sqrt{s}/20$ cut for all particles to suppress non-resonant backgrounds. At $\sqrt{s} = 14$ TeV, we get a sensitivity to $|\Delta a_\tau| \approx 6 \times 10^{-4}$, which is weaker than the other considered channels, but

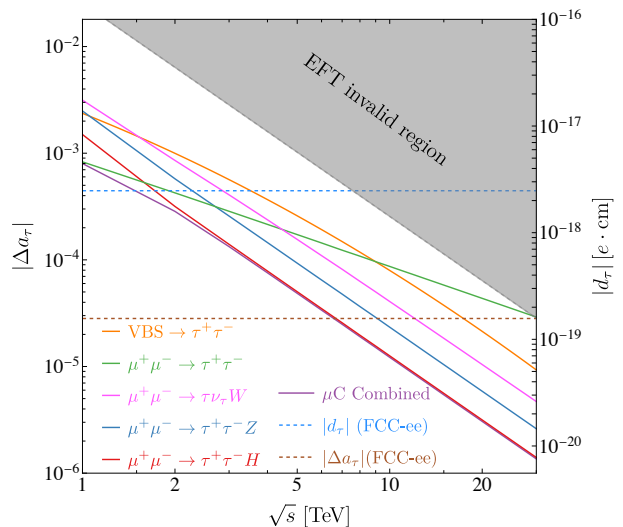


FIG. 4. 95% CL bounds on Δa_τ and d_τ at multi-TeV muon collider as a function of \sqrt{s} , assuming real $\mathcal{C}_{\tau B}$ and $\mathcal{C}_{\tau W}$. The grey region denotes perturbative unitarity violation in Eq. (2).

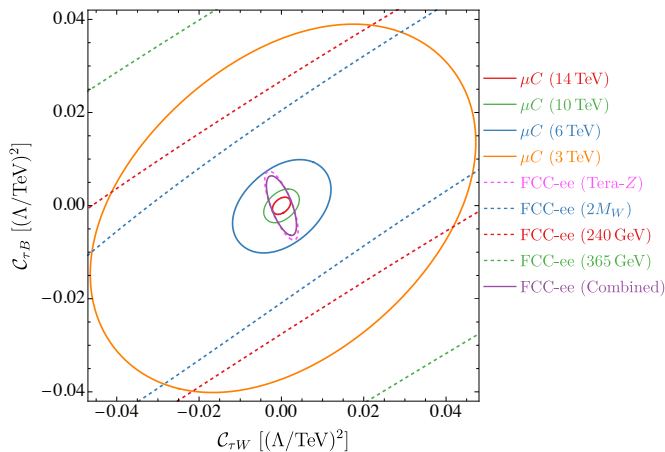


FIG. 5. 95% CL bounds in the $(C_{\tau W}, C_{\tau B})$ plane at FCC-ee and multi-TeV muon collider. The bounds scale as $(\Lambda/\text{TeV})^2$ and assume real $C_{\tau W}$ and $C_{\tau B}$.

comparable to the prospects for FCC-ee.

Figure 5 shows the 95% CL bounds in the $(C_{\tau W}, C_{\tau B})$ plane at FCC-ee and at a multi-TeV μC . A clear pattern emerges: while FCC-ee provides strong constraints on a_τ^Z and d_τ^Z from the high-luminosity Z -pole program, the μC becomes the more powerful probe of both $a_\tau^{(Z)}$ and $d_\tau^{(Z)}$ at energies above ~ 10 TeV. In particular, a 14 TeV μC improves the constraint on d_τ by more than two orders of magnitude relative to FCC-ee.

V. CONCLUSIONS

In this Letter, we have shown that future lepton colliders can improve current experimental sensitivities to τ dipole moments by several orders of magnitude.

Owing to the extremely high luminosity and clean environment of FCC-ee, $\gamma\gamma \rightarrow \tau^+\tau^-$ provides the most stringent bound on the anomalous magnetic moment, $|\Delta a_\tau| \lesssim 3.0 \times 10^{-5}$ (see Table III), while $e^+e^- \rightarrow \tau^+\tau^-$ yields the strongest constraints on the electric dipole moment, $|d_\tau| \lesssim 2.5 \times 10^{-18} e \text{ cm}$, and on the weak dipole moments, $|\Delta a_\tau^Z| \lesssim 1.0 \times 10^{-5}$ and $|d_\tau^Z| \lesssim 4.4 \times 10^{-19} e \text{ cm}$ (see Table II). The energy growth of associated Higgs production $\mu^+\mu^- \rightarrow \tau^+\tau^-H$ at a multi-TeV muon collider makes this process the most sensitive probe of τ dipole operators. At center-of-mass energies around 14 TeV, the resulting bound on Δa_τ (d_τ) improves by one (two) order(s) of magnitude relative to FCC-ee (see Fig. 4).

Our results indicate that future lepton colliders offer a promising opportunity to probe the τ dipole moments, underscoring the complementarity of FCC-ee and a multi-TeV muon collider. They further motivate dedicated studies of the systematic uncertainties not included in the present analysis.

Acknowledgments: We thank B. Batell, I. Brivio, C. Degrande, G. Durieux, T. Han, M. Hoferichter, F. Jaffredo, J. Liu, O. Mattelaer, M. Passera, and X. Wang for useful discussions. This research is partially supported by the IISN convention 4.4517.08, “Theory of fundamental interactions.” Y. Ma acknowledges the support as a Postdoctoral Fellow of the Fond de la Recherche Scientifique de Belgique (F.R.S.-FNRS), Belgium. Computational resources have been provided by the supercomputing facilities of the Université catholique de Louvain (CISM/UCL) and the Consortium des Équipements de Calcul Intensif en Fédération Wallonie Bruxelles (CÉCI) funded by the Fond de la Recherche Scientifique de Belgique (F.R.S.-FNRS) under convention 2.5020.11 and by the Walloon Region. G. Levati gratefully acknowledges financial support by the Swiss National Science Foundation (Project No. TMC2G-2_213690). Z.Q. Wang acknowledges support from the China Scholarship Council (CSC)- UCLouvain Co-funding PhD Fellowship (Grant No. 202206040017). P. Paradisi received funding by the European Union’s Horizon 2020 research and innovation programme under the Marie Skłodowska-Curie grant agreements n. 860881 - HIDDeN, n. 101086085 - ASYMMETRY, by the Italian MUR Departments of Excellence grant 2023-2027 “Quantum Frontiers” and by the European Union - Next Generation EU and by the Italian Ministry of University and Research (MUR) via the PRIN 2022 project n. 2022K4B58X - AxionOrigins. D. Buttazzo is partially funded by the European Union - Next Generation EU and MUR through the grant PRIN 202289JEW4. We also acknowledge support from the COMETA COST Action CA22130.

-
- [1] X. Fan, T. G. Myers, B. A. D. Sukra, and G. Gabrielse, Measurement of the Electron Magnetic Moment, *Phys. Rev. Lett.* **130**, 071801 (2023), arXiv:2209.13084 [physics.atom-ph].
 - [2] D. P. Aguillard *et al.* (Muon $g-2$), Measurement of the Positive Muon Anomalous Magnetic Moment to 0.20 ppm, *Phys. Rev. Lett.* **131**, 161802 (2023), arXiv:2308.06230 [hep-ex].
 - [3] D. P. Aguillard *et al.* (Muon $g-2$), Measurement of the Positive Muon Anomalous Magnetic Moment to 127 ppb, *Phys. Rev. Lett.* **135**, 101802 (2025), arXiv:2506.03069 [hep-ex].
 - [4] L. Morel, Z. Yao, P. Cladé, and S. Guellati-Khélifa, Determination of the fine-structure constant with an accuracy of 81 parts per trillion, *Nature* **588**, 61 (2020).
 - [5] R. H. Parker, C. Yu, W. Zhong, B. Estey, and H. Müller, Measurement of the fine-structure constant as a test of the Standard Model, *Science* **360**, 191 (2018), arXiv:1812.04130 [physics.atom-ph].
 - [6] R. Aliberti *et al.*, The anomalous magnetic moment of the muon in the Standard Model: an update, *Phys. Rept.*

- 1143**, 1 (2025), arXiv:2505.21476 [hep-ph].
- [7] D. W. Hertzog and M. Hoferichter, The anomalous magnetic moment of the muon: status and perspectives, arxiv 10.1146/annurev-nucl-102422-040841 (2025), arXiv:2512.16980 [hep-ph].
- [8] T. S. Roussy *et al.*, An improved bound on the electron's electric dipole moment, *Science* **381**, adg4084 (2023), arXiv:2212.11841 [physics.atom-ph].
- [9] G. W. Bennett *et al.* (Muon $g - 2$), An Improved Limit on the Muon Electric Dipole Moment, *Phys. Rev. D* **80**, 052008 (2009), arXiv:0811.1207 [hep-ex].
- [10] S. Eidelman and M. Passera, Theory of the tau lepton anomalous magnetic moment, *Mod. Phys. Lett. A* **22**, 159 (2007), arXiv:hep-ph/0701260.
- [11] S. Eidelman, D. Epifanov, M. Fael, L. Mercolli, and M. Passera, τ dipole moments via radiative leptonic τ decays, *JHEP* **03**, 140, arXiv:1601.07987 [hep-ph].
- [12] L. Di Luzio, A. Keshavarzi, A. Masiero, and P. Paradisi, Model-Independent Tests of the Hadronic Vacuum Polarization Contribution to the Muon $g-2$, *Phys. Rev. Lett.* **134**, 011902 (2025), arXiv:2408.01123 [hep-ph].
- [13] M. Hoferichter, P. Stoffer, and M. Zillinger, Hadronic light-by-light scattering in the anomalous magnetic moments of electron and τ , *Phys. Lett. B* **866**, 139565 (2025), arXiv:2504.10582 [hep-ph].
- [14] H. Wittig, Lepton anomalous magnetic moments: Theory, arxiv (2025), arXiv:2512.18382 [hep-ph].
- [15] R. Barbieri, G. R. Dvali, and L. J. Hall, Predictions from a $U(2)$ flavor symmetry in supersymmetric theories, *Phys. Lett. B* **377**, 76 (1996), arXiv:hep-ph/9512388.
- [16] R. Barbieri and L. J. Hall, A Grand unified supersymmetric theory of flavor, *Nuovo Cim. A* **110**, 1 (1997), arXiv:hep-ph/9605224.
- [17] R. Barbieri, L. J. Hall, S. Raby, and A. Romanino, Unified theories with $U(2)$ flavor symmetry, *Nucl. Phys. B* **493**, 3 (1997), arXiv:hep-ph/9610449.
- [18] R. Barbieri, L. J. Hall, and A. Romanino, Consequences of a $U(2)$ flavor symmetry, *Phys. Lett. B* **401**, 47 (1997), arXiv:hep-ph/9702315.
- [19] A. L. Kagan, G. Perez, T. Volansky, and J. Zupan, General Minimal Flavor Violation, *Phys. Rev. D* **80**, 076002 (2009), arXiv:0903.1794 [hep-ph].
- [20] R. Barbieri, D. Buttazzo, F. Sala, and D. M. Straub, Flavour physics from an approximate $U(2)^3$ symmetry, *JHEP* **07**, 181, arXiv:1203.4218 [hep-ph].
- [21] G. Panico and A. Wulzer, *The Composite Nambu-Goldstone Higgs*, Vol. 913 (Springer, 2016) arXiv:1506.01961 [hep-ph].
- [22] G. Panico and A. Pomarol, Flavor hierarchies from dynamical scales, *JHEP* **07**, 097, arXiv:1603.06609 [hep-ph].
- [23] R. Barbieri, D. Buttazzo, F. Sala, D. M. Straub, and A. Tesi, A 125 GeV composite Higgs boson versus flavour and electroweak precision tests, *JHEP* **05**, 069, arXiv:1211.5085 [hep-ph].
- [24] A. Glioti, R. Rattazzi, L. Ricci, and L. Vecchi, Exploring the flavor symmetry landscape, *SciPost Phys.* **18**, 201 (2025), arXiv:2402.09503 [hep-ph].
- [25] M. Bordone, C. Cornella, J. Fuentes-Martin, and G. Isidori, A three-site gauge model for flavor hierarchies and flavor anomalies, *Phys. Lett. B* **779**, 317 (2018), arXiv:1712.01368 [hep-ph].
- [26] J. Fuentes-Martin, G. Isidori, J. M. Lizana, N. Selimovic, and B. A. Stefanek, Flavor hierarchies, flavor anomalies, and Higgs mass from a warped extra dimension, *Phys. Lett. B* **834**, 137382 (2022), arXiv:2203.01952 [hep-ph].
- [27] J. Davighi and G. Isidori, Non-universal gauge interactions addressing the inescapable link between Higgs and flavour, *JHEP* **07**, 147, arXiv:2303.01520 [hep-ph].
- [28] W. Buchmuller and D. Wyler, Effective Lagrangian Analysis of New Interactions and Flavor Conservation, *Nucl. Phys. B* **268**, 621 (1986).
- [29] J. Abdallah *et al.* (DELPHI), Study of tau-pair production in photon-photon collisions at LEP and limits on the anomalous electromagnetic moments of the tau lepton, *Eur. Phys. J. C* **35**, 159 (2004), arXiv:hep-ex/0406010.
- [30] G. Aad *et al.* (ATLAS), A measurement of the high-mass $\tau\bar{\tau}$ production cross-section at $\sqrt{s} = 13$ TeV with the ATLAS detector and constraints on new particles and couplings, *JHEP* **10**, 054, arXiv:2503.19836 [hep-ex].
- [31] A. Hayrapetyan *et al.* (CMS), Observation of $\gamma\gamma \rightarrow \tau\tau$ in proton-proton collisions and limits on the anomalous electromagnetic moments of the τ lepton, *Rept. Prog. Phys.* **87**, 107801 (2024), arXiv:2406.03975 [hep-ex].
- [32] K. Inami *et al.* (Belle), An improved search for the electric dipole moment of the τ lepton, *JHEP* **04**, 110, arXiv:2108.11543 [hep-ex].
- [33] J. Bernabeu, G. A. Gonzalez-Sprinberg, and J. Vidal, CP violation and electric-dipole-moment at low energy tau production with polarized electrons, *Nucl. Phys. B* **763**, 283 (2007), arXiv:hep-ph/0610135.
- [34] J. Bernabeu, G. A. Gonzalez-Sprinberg, J. Papavassiliou, and J. Vidal, Tau anomalous magnetic moment form-factor at super B/flavor factories, *Nucl. Phys. B* **790**, 160 (2008), arXiv:0707.2496 [hep-ph].
- [35] J. Bernabeu, G. A. Gonzalez-Sprinberg, and J. Vidal, Tau spin correlations and the anomalous magnetic moment, *JHEP* **01**, 062, arXiv:0807.2366 [hep-ph].
- [36] A. Crivellin, M. Hoferichter, and J. M. Roney, Toward testing the magnetic moment of the tau at one part per million, *Phys. Rev. D* **106**, 093007 (2022), arXiv:2111.10378 [hep-ph].
- [37] D. M. Asner *et al.* (US Belle II Group, Belle II/SuperKEKB e- Polarization Upgrade Working Group), Snowmass 2021 White Paper on Upgrading SuperKEKB with a Polarized Electron Beam: Discovery Potential and Proposed Implementation, in *Snowmass 2021* (2022) arXiv:2205.12847 [physics.acc-ph].
- [38] H. Aihara *et al.*, The Belle II Detector Upgrades Framework Conceptual Design Report (2024), arXiv:2406.19421 [hep-ex].
- [39] J. Gogniat, M. Hoferichter, and Y. Ulrich, Towards testing $(g - 2)_\tau$ in $e^+e^- \rightarrow \tau^+\tau^-$: radiative corrections and projections for Belle II, *JHEP* **07**, 172, arXiv:2505.09678 [hep-ph].
- [40] M. Hoferichter and G. Levati, Light new physics and the τ lepton dipole moments (2025), arXiv:2511.03786 [hep-ph].
- [41] M. Hoferichter and G. Levati, Light new physics and the τ lepton dipole moments: prospects at Belle II (2025), arXiv:2510.13966 [hep-ph].
- [42] W. Altmannshofer *et al.* (Belle II), The Belle II Physics Book, *PTEP* **2019**, 123C01 (2019), [Erratum: *PTEP* **2020**, 029201 (2020)], arXiv:1808.10567 [hep-ex].
- [43] A. Abada *et al.* (FCC), FCC-ee: The Lepton Collider: Future Circular Collider Conceptual Design Report Volume 2, *Eur. Phys. J. ST* **228**, 261 (2019).
- [44] G. Bernardi *et al.*, The Future Circular Collider: a

- Summary for the US 2021 Snowmass Process, (2022), [arXiv:2203.06520 \[hep-ex\]](#).
- [45] M. Benedikt *et al.* (FCC), Future Circular Collider Feasibility Study Report: Volume 1, Physics, Experiments, Detectors, *Eur. Phys. J. C* **85**, 1468 (2025), [arXiv:2505.00272 \[hep-ex\]](#).
- [46] J. Altmann *et al.*, *ECFA Higgs, electroweak, and top Factory Study*, CERN Yellow Reports: Monographs, Vol. 5/2025 (2025) [arXiv:2506.15390 \[hep-ex\]](#).
- [47] J. de Blas *et al.* (Muon Collider), The physics case of a 3 TeV muon collider stage, *arxiv* (2022), [arXiv:2203.07261 \[hep-ph\]](#).
- [48] C. Aime *et al.*, Muon Collider Physics Summary, *arxiv* (2022), [arXiv:2203.07256 \[hep-ph\]](#).
- [49] K. M. Black *et al.*, Muon Collider Forum report, *JINST* **19** (02), T02015, [arXiv:2209.01318 \[hep-ex\]](#).
- [50] C. Accettura *et al.*, Towards a muon collider, *Eur. Phys. J. C* **83**, 864 (2023), [Erratum: *Eur.Phys.J.C* 84, 36 (2024)], [arXiv:2303.08533 \[physics.acc-ph\]](#).
- [51] J. P. Delahaye, M. Diemoz, K. Long, B. Mansoulié, N. Pastrone, L. Rivkin, D. Schulte, A. Skrinsky, and A. Wulzer, Muon Colliders, *arxiv* (2019), [arXiv:1901.06150 \[physics.acc-ph\]](#).
- [52] N. Bartosik *et al.*, Detector and Physics Performance at a Muon Collider, *JINST* **15** (05), P05001, [arXiv:2001.04431 \[hep-ex\]](#).
- [53] D. Schulte, J.-P. Delahaye, M. Diemoz, K. Long, B. Mansoulié, N. Pastrone, L. Rivkin, A. Skrinsky, and A. Wulzer, Prospects on Muon Colliders, *PoS ICHEP2020*, 703 (2021).
- [54] K. Long, D. Lucchesi, M. Palmer, N. Pastrone, D. Schulte, and V. Shiltsev, Muon colliders to expand frontiers of particle physics, *Nature Phys.* **17**, 289 (2021), [arXiv:2007.15684 \[physics.acc-ph\]](#).
- [55] D. Stratakis *et al.* (Muon Collider), A Muon Collider Facility for Physics Discovery, *arxiv* (2022), [arXiv:2203.08033 \[physics.acc-ph\]](#).
- [56] N. Bartosik *et al.* (Muon Collider), Simulated Detector Performance at the Muon Collider, *arxiv* (2022), [arXiv:2203.07964 \[hep-ex\]](#).
- [57] S. Jindariani *et al.* (Muon Collider), Promising Technologies and R&D Directions for the Future Muon Collider Detectors, *arxiv* (2022), [arXiv:2203.07224 \[physics.ins-det\]](#).
- [58] C. Accettura *et al.* (International Muon Collider), The Muon Collider, *arxiv* (2025), [arXiv:2504.21417 \[physics.acc-ph\]](#).
- [59] D. Buttazzo and P. Paradisi, Probing the muon $g - 2$ anomaly with the Higgs boson at a muon collider, *Phys. Rev. D* **104**, 075021 (2021), [arXiv:2012.02769 \[hep-ph\]](#).
- [60] B. Grzadkowski, M. Iskrzynski, M. Misiak, and J. Rosiek, Dimension-Six Terms in the Standard Model Lagrangian, *JHEP* **10**, 085, [arXiv:1008.4884 \[hep-ph\]](#).
- [61] L. Allwicher, L. Di Luzio, M. Fedele, F. Mescia, and M. Nardecchia, What is the scale of new physics behind the muon $g-2$?, *Phys. Rev. D* **104**, 055035 (2021), [arXiv:2105.13981 \[hep-ph\]](#).
- [62] L. C. Bresciani, P. Paradisi, and A. Sainaghi, Unitarity bounds and sum rules in the SMEFT, *arxiv* (2026), [arXiv:2603.03423 \[hep-ph\]](#).
- [63] E. E. Jenkins, A. V. Manohar, and M. Trott, Renormalization Group Evolution of the Standard Model Dimension Six Operators I: Formalism and lambda Dependence, *JHEP* **10**, 087, [arXiv:1308.2627 \[hep-ph\]](#).
- [64] E. E. Jenkins, A. V. Manohar, and M. Trott, Renormalization Group Evolution of the Standard Model Dimension Six Operators II: Yukawa Dependence, *JHEP* **01**, 035, [arXiv:1310.4838 \[hep-ph\]](#).
- [65] R. Alonso, E. E. Jenkins, A. V. Manohar, and M. Trott, Renormalization Group Evolution of the Standard Model Dimension Six Operators III: Gauge Coupling Dependence and Phenomenology, *JHEP* **04**, 159, [arXiv:1312.2014 \[hep-ph\]](#).
- [66] E. E. Jenkins, A. V. Manohar, and P. Stoffer, Low-Energy Effective Field Theory below the Electroweak Scale: Anomalous Dimensions, *JHEP* **01**, 084, [Erratum: *JHEP* **12**, 042 (2023)], [arXiv:1711.05270 \[hep-ph\]](#).
- [67] J. Aebischer, W. Dekens, E. E. Jenkins, A. V. Manohar, D. Sengupta, and P. Stoffer, Effective field theory interpretation of lepton magnetic and electric dipole moments, *JHEP* **07**, 107, [arXiv:2102.08954 \[hep-ph\]](#).
- [68] G. F. Giudice, P. Paradisi, and M. Passera, Testing new physics with the electron $g-2$, *JHEP* **11**, 113, [arXiv:1208.6583 \[hep-ph\]](#).
- [69] W. J. Marciano, A. Masiero, P. Paradisi, and M. Passera, Contributions of axionlike particles to lepton dipole moments, *Phys. Rev. D* **94**, 115033 (2016), [arXiv:1607.01022 \[hep-ph\]](#).
- [70] J. Alda, G. Levati, P. Paradisi, S. Rigolin, and N. Selimovic, Collider and astrophysical signatures of light scalars with enhanced τ couplings, *JHEP* **06**, 008, [arXiv:2407.18296 \[hep-ph\]](#).
- [71] S. Frixione, M. L. Mangano, P. Nason, and G. Ridolfi, Improving the Weizsacker-Williams approximation in electron - proton collisions, *Phys. Lett. B* **319**, 339 (1993), [arXiv:hep-ph/9310350](#).
- [72] J. M. Cornwall, D. N. Levin, and G. Tiktopoulos, Derivation of Gauge Invariance from High-Energy Unitarity Bounds on the s Matrix, *Phys. Rev. D* **10**, 1145 (1974), [Erratum: *Phys.Rev.D* 11, 972 (1975)].
- [73] B. W. Lee, C. Quigg, and H. B. Thacker, Weak Interactions at Very High-Energies: The Role of the Higgs Boson Mass, *Phys. Rev. D* **16**, 1519 (1977).
- [74] M. S. Chanowitz and M. K. Gaillard, The TeV Physics of Strongly Interacting W's and Z's, *Nucl. Phys. B* **261**, 379 (1985).
- [75] T. Han, Y. Ma, and K. Xie, Quark and gluon contents of a lepton at high energies, *JHEP* **02**, 154, [arXiv:2103.09844 \[hep-ph\]](#).